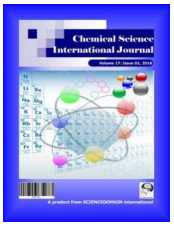

Chemical Science International Journal
17(2): 1-10, 2016, Article no.CSIJ.29509
Previously known as American Chemical Science Journal
ISSN: 2249-0205

SCIENCEDOMAIN *international*
www.sciencedomain.org

Ion Exchange Kinetics of Mg(II) from Aqueous Solutions with 732 Cation-exchange Resin

Jia Qian[1], Yiwen Liu[1], Weilan Xue[1] and Zuoxiang Zeng[1*]

[1]Institute of Chemical Engineering, East China University of Science and Technology, Shanghai 200237, China.

Authors' contributions

This work was carried out in collaboration between all authors. Author JQ designed the study, wrote the protocol and wrote the first draft of the manuscript. Author ZZ reviewed the experimental design and all drafts of the manuscript. Authors JQ and YL managed the analyses of the study. Author WX identified the plants. Authors YL and WX performed the statistical analysis. All authors read and approved the final manuscript.

Article Information

DOI: 10.9734/CSIJ/2016/29509
Editor(s):
(1) Georgiy B. Shul'pin, Semenov Institute of Chemical Physics, Russian Academy of Sciences, Moscow, Russia.
Reviewers:
(1) Ali Mahmoud Ahmed Abdullah, Alexandria University, Egypt.
(2) Le Van Tan, Industrial University, Ò Hochiminh City, Vietnam.
(3) Nasr Abdelaziz Abdelfattah, Nuclear Materials Authority, El Maadi, Cairo, Egypt.
Complete Peer review History: http://www.sciencedomain.org/review-history/16703

Original Research Article

Received 15th September 2016
Accepted 16th October 2016
Published 28th October 2016

ABSTRACT

The hydrogen type sulfonic resin 732 cation-exchange resin (732-CR) was applied to exchange Mg(II) from aqueous solution. The ion exchange kinetics were studied in batch experiments at temperature range of 298-328 K and Mg(II) concentration range of 5-40 mol·m^{-3}. The kinetic data were first treated by Nernst-Planck equation for the exchange of univalent and bivalent ions, and also treated and compared by shrinking-core model that takes into account diffusion of metal ions within resin pores. The values and relationships of diffusion coefficients of counter ions (D_M and D_H) and effective diffusion coefficients of magnesium ions (D_e) were evaluated and discussed. Other useful ion exchange kinetic parameters such as self-diffusion coefficient (D_0), energy of activation (ΔE_a) and entropy of activation (ΔS^*) were evaluated. The results show that the ion exchange process is favored under particle diffusion control mechanism and above two models can both describe kinetics of the removal of Mg(II) from aqueous solution by 732-CR.

**Corresponding author: E-mail: zengzx@ecust.edu.cn;*

Keywords: Ion exchange kinetics; magnesium ions; 732 cation-exchange resin; Nernst-planck equation; shrinking-core model.

NOMENCLATURES

$C_{M,e}$: Equilibrium concentrations of Mg(II) in solution, mol·m^{-3}
$C_{M,t}$: Centration of Mg(II) at time t in solution, mol·m^{-3}
$C_{M,0}$: Initial concentration of Mg(II) in solution, mol·m^{-3}
D_e : Effective diffusion coefficient of M^{2+} within the resin, m^2·s^{-1}
D_o : Self-diffusion coefficient of M^{2+}, calculated by Nernst-Planck equation, m^2·s^{-1}
D_o' : Self-diffusion coefficient of M^{2+}, calculated by shrinking-core model, m^2·s^{-1}
D_H : Inter diffusion coefficient of counter ion H^+, m^2·s^{-1}
D_M : Inter diffusion coefficient of counter ion M^{2+}, m^2·s^{-1}
D_{HM} : Coupled interdiffusion coefficient, m^2·s^{-1}
d : Ionic jump distance, m
ΔE_a : Energy of activation, calculated by Nernst-Planck model, kJ·mol^{-1}
ΔE_a' : Energy of activation, calculated by shinking-core model, kJ·mol^{-1} shrinking
h : Plank's constant
q_e : Equilibrium exchange capacity, mol·m^{-3}
r_c : Radius of the interface of unreacted core, m
r_0 : Particle radius, m
ΔS^* : Entropy of activation, calculated by Nernst-Planck model, J·mol^{-1}·K^{-1}
ΔS^*' : Entropy of activation, calculated by shinking-core model, J·mol^{-1}·K^{-1} shrinking
T : Absolute temperature, K
V : Volume of the solution, m^3
W : Weight of dried resin, kg
$X(t)$, $U(\tau)$: Fractional attainment of equilibrium
Z_H/Z_M : Charge ratio
a : Mobility ratio
k : Boltzmann constant
ρ_s : Density of dried resin, kg·m^{-3}
τ : Dimensionless time parameter

1. INTRODUCTION

Magnesium and calcium concentrations, which represent the hardness of water, are present in most natural waters. Hard water can result in serious problems both in industrial and domestic settings. It can cause scaling in different industrial operators such as hot water tanks, boilers, washing machines and cooling towers that reduce power output and thermal efficiency [1-4]. It can foul pipeline and membrance [5-7], as well as prevent soaps from lathering [8]. Moreover, in some industry processes, it's essential to remove alkaline-earth metal ions in order to obtain pure chemicals, increase productive efficiency and avoid potential dangers [9,10]. Therefore, softening or removal of hardness cations from groundwater and surface water is required from the points of economy, safety and human health.

Lime softening and ion exchange softening are two common methods for the removal of hardness [3,4,11] along with nanofiltration, membrane processes, electrochemical techniques, reverse osmosis, and biological processes [12-16]. Compared to the drawbacks of the lime method include the production of a high volume of sludge stream and excessive use of chemicals [17], the advantages of ion exchange include effectiveness, selectivity, recovery, fewer precipitation, and better economics in water softening [18-20]. 732 cation-exchange resin (732-CR), a gel-type polystyrene sulphonated strong cation-exchange resin, is widely produced and used as an ion-exchanger as its high exchange capacity and relative low cost [21]. However, no detailed kinetic and equilibrium studies for this resin as H^+ form for the ion exchange of alkaline-earth metals from aqueous solution.

Ion exchange kinetics envisage the mechanism of ion exchange, rate determining step and the rate laws obeyed by the ion exchange system [22]. It has an important role in the selection of

exchangers and exchange conditions in a certain application and in the evaluation of the performance of ion exchange process. Batch ion exchange techniques are performed to obtain the distribution function of a solute between the exchanger and solution phase.

In this study, 732-CR as H^+ form was evaluated from the kinetic points of view for Mg(II) removal by ion exchange. The parameters that influence ion exchange, such as contact time, temperature and initial concentration of Mg(II) were investigated. The kinetic data were described by different kinetic models: Nernst-Planck equation and shrinking core model (SCM). The mechanism and rate determining step of ion exchange were studied by both models. In addition, the equilibrium, kinetics parameters and the relationship between these two kinetic models were evaluated from the ion exchange measurements.

2. EXPERIMENTAL

2.1 Materials and Apparatus

Material: 732-CR in sodium form (Shanghai Resin Factory). Its physicochemical properties and specification as reported are listed in Table 1. Magnesium chloride, basic magnesium carbonate, ethylene diamine tetra acetic acid, disodium salt (EDTA) and Eriochrome black T, (analytical grade, Sinopharm Chemical Reagent Co. Ltd.); Hydrochloric acid (35%), (Shanghai Lingfeng Chemical Reagent Co. Ltd.).

Apparatus: Drying oven (GZX-9070MEB); Water bath constant temperature oscillator (DF-101S).

Table 1. Characteristics of 732-CR

Characteristics	Value
Matrix	Styrene – divinyl benzene copolymer
Functional group	Sulfonic acid
Physical form	Transparent, claybank beads
Ionic forms as shipped	Na^+
Total exchange capacity	≥4.60 mmol/l
Particle size	0.3-1.25 mm
Water content	45-53%
Specific gravity	1.19-1.29
pH range	1-14

2.2 Methods

2.2.1 Preparation of H^+ form ion-exchange resin

The resin was washed with demineralized water (DMW) to remove impurities and dried at 338 K to constant weight. Sample sifters of 40 mesh and 50 mesh were used to sieve the dried resin to obtain particles of particular size range (~182 μm). The selected 732-CR in Na^+ form was converted to H^+ form by agitating with 1 M HCl for 24 h, and intermittently replacing the supernatant liquid with fresh acid. The excess acid was removed after several washings with DMW until the final washing became neutral. Finally the resin was dried at 338 K and stored in a desiccator for further experimental studies.

2.2.2 Batch kinetic experiments

The exchange kinetic experiments were carried out in 250 mL conical flasks as follows: 50±0.1 mL Mg(II) solutions were shaken with 0.2±0.001 g of the dried H^+ form resin at different temperatures (298-328 K) and different initial Mg(II) concentrations (5-40 $mol \cdot m^{-3}$). Determination of the temperature was estimated to be accurate to ±0.1 K and the standard uncertainties of initial Mg(II) concentration are 2%. The minimum stirring speed was determined and above which the kinetics are independent of the agitation. The agitated batch experiments were carried at a shaking speed above this minimum speed. At desired time intervals (0.5, 1, 2, ect. to 720 min), the supernatant liquid was removed immediately and titrated by EDTA. All the experimental studies were carried out three times and the mean values were taken for calculation.

3. RESULTS AND DISCUSSION

3.1 Kinetic Results

3.1.1 Effect of contact time

The extents of ion exchange are expressed in terms of the fractional attainment of equilibrium, $X(t)$, according to the equation:

$$X(t) = \frac{C_{M,0} - C_M}{C_{M0} - C_{M,e}} = \frac{\text{the amount of exchange at time 't'}}{\text{the amount of exchange at equilibrium}} \quad (1)$$

where $C_{M,0}$, C_M, and $C_{M,e}$, are the concentration of Mg(II) at time 0, t, and equilibrium in the aqueous phase respectively.

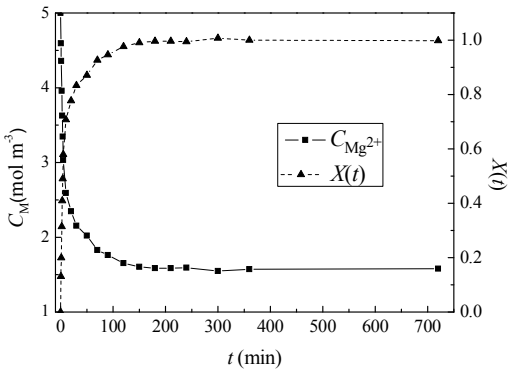

Fig. 1. Effect of contact time on ion exchange of Mg(II) with 732-CR (initial Mg(II) concentration: 5 mol·m^{-3}; temperature: 308 K)

Fig. 1 shows the effect of contact time on the ion exchange of Mg(II) with 732-CR. It is clear that the removal of Mg(II) increases with the lapse of time. The fractional attainment of equilibrium increases rapidly during a few minutes at first, and then increases slowly until the equilibrium state is reached. The figure reveals that 360 min is enough for the establishment of equilibrium for initial Mg(II) concentration of 5 mol·m^{-3} at 308 K. Therefore, 360 min is assumed to be the equilibrium time of ion exchange for all systems. The initial ion exchange rate was very fast may be due to the existence of greater number of resin sites available for the exchange of metal ions. As the remaining vacant sites decreasing on the surface, the ion exchange rate slowed.

3.1.2 Effect of temperature

Fig. 2 is the plots of $X(t)$ *versus* t for Mg^{2+}-H^+ exchanges at four different temperatures. It is shown that the removal of Mg(II) is favored with the increase in temperature. This may be attributed to the increase in ion mobility and the decrease in solution viscosity with the increase in temperature, which boost the velocity of the ions moving across the liquid-solid boundary layer to the solid surface [21-23].

3.1.3 Effect of initial concentration of Mg(II)

Two physical and one chemical kinetic mechanisms are normally involved in ion exchange processes. The (chemical) ion-exchange reaction is normally much faster than the (physical) mass transfer phenomena. This is why only the external (film) and the internal (particle) diffusion are considered. The concentration effect on the mechanism of exchange was studied at 308 K. Plots of $X(t)$ *versus* t (Fig. 3a) indicate that the rate of exchange is proportional to the initial Mg(II) concentration. As the previous works indicate, a particle diffusion controlled process is favored by a high metal ion concentration, relatively large particle size of the exchanger and a vigorous shaking of the exchanging mixture [24]. According to the Nernst-Planck equation (Eq. (3)), each fractional attainment of equilibrium has a corresponding value of τ. The plots of τ *versus* t (Fig. 3b) are straight lines passing through the origin at and above 20 mol·m^{-3} of initial Mg(II) concentration, confirming the particle diffusion controlled phenomenon [25,26]. According to the concentration effect on the rate of ion exchange, kinetic measurements were made at 0.02 M initial Mg(II) concentration.

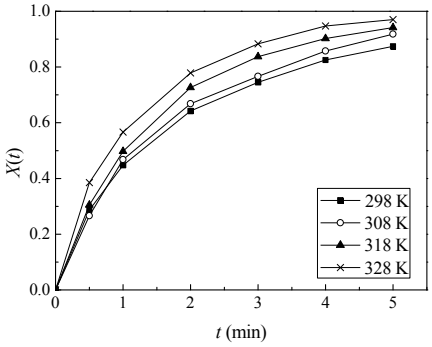

Fig. 2. Effect of temperature on ion exchange of Mg(II) with 732-CR (initial Mg(II) concentration: 20 mol·m^{-3})

3.2 Kinetic Models

Different models have been used to describe the kinetics of ion-exchange between metallic solutes and an exchanger. In this work, the application of kinetic models to fit experimental results was demonstrated using Nernst-Planck equation and shrinking core model in the system of Mg^{2+}-H^+ exchange in sulphonic cationic resin.

3.2.1 Nernst-Planck equation

The Nernst-Planck equation can be used to solve the particle diffusion control ion exchange process with the following assumptions given by Helfrich [27,28]: The individual diffusion coefficients are essentially constant for a given resin; the concentration of fixed ionic groups throughout the resin remains unchanged; and the

presence of co-ions in the resin and the swelling condition of the resin are neglected.

The exchange of bivalent metals M^{2+} with the resin in H^+ form is essentially a process of M^{2+} diffusing into and H^+ diffusing out of the resin phase, and H^+ being substituted by an equivalent amount of M^{2+}. Hence the coupled interdiffusion coefficient D_{HM} can be written as [29]:

$$D_{HM} = \frac{D_H D_M (Z_H^2 C_H + Z_M^2 C_M)}{Z_H^2 C_H D_H + Z_M^2 C_M D_M} \quad (2)$$

D_{HM} depends on the relative concentration of the exchanging species (H^+ and M^{2+}) in the resin. Since initially $C_H > C_M$, D_{HM} approximately equals to the value of D_M. On the basis of the Nernst-Planck equation, the numerical results can be expressed by explicit approximation [27,28]:

$$U(\tau) = \{1 - \exp[\pi^2 (f_1(\alpha)\tau + f_2(\alpha)\tau^2 + f_3(\alpha)\tau^3)]\}^{1/2} \quad (3)$$

where $U(\tau)$ equals to the fractional attainment of equilibrium, $X(t)$, τ is the half time of exchange, a dimensionless time parameter, and α is the mobility ratio as shown in Eq. (4) to (6).

$$U(\tau) = X(t) \quad (4)$$

$$\tau = D_M t / r_0^2 \quad (5)$$

$$\alpha = D_H / D_M \quad (6)$$

D_H and D_M are the interdiffusion coefficients of counter ions H^+ and M^{2+} in the resin phase and r_0 is the particle radius. The three functions $f_1(\alpha)$, $f_2(\alpha)$ and $f_3(\alpha)$ depend on the mobility ratio (α) and the charge ratio (Z_H/Z_M) of the exchanging ions. When the exchanger is taken in the H^+-form and the exchanging ion is M^{2+}, for $1 \le \alpha \le 20$, the three functions have the values:

$$f_1(\alpha) = -\frac{1}{0.64 + 0.36\alpha^{0.668}} \quad (7)$$

$$f_2(\alpha) = -\frac{1}{0.96 - 2.0\alpha^{0.4635}} \quad (8)$$

$$f_3(\alpha) = -\frac{1}{0.27 + 0.09\alpha^{1.140}} \quad (9)$$

The τ values of the ion exchange processes are obtained by solving Eq. (3) using a computer, and the results also given the α value. The plots of τ *versus* t at four different temperatures for the ion exchange of Mg(II) with 732-CR are shown in Fig. 4.

The slopes (S_1) of τ *versus* t plots are calculated using a linear regression model; the data are summarized in Table 2. According to Eq. (5) and (6), we can obtain D_M and D_H values, which are listed in Table 3.

An Arrhenius plot as shown in Fig. 5 could be used to show the temperature dependence of the diffusion coefficient of metal ions (D_M) following the Arrhenius equation:

$$D_M = D_0 \exp\left(\frac{-\Delta E_a}{RT}\right) \quad (10)$$

where ΔE_a is the activation energy of the diffusion process, R is the gas constant, T is the absolute temperature, and D_0 is the pre-exponential constant, self-diffusion coefficient of M^{2+}. The plot of log D_M against $1/T$ for ion exchange of Mg(II) with 732-CR (Fig. 5) results in a straight line. The intercept and the slope values give the value of D_0 and ΔE_a (Table 4).

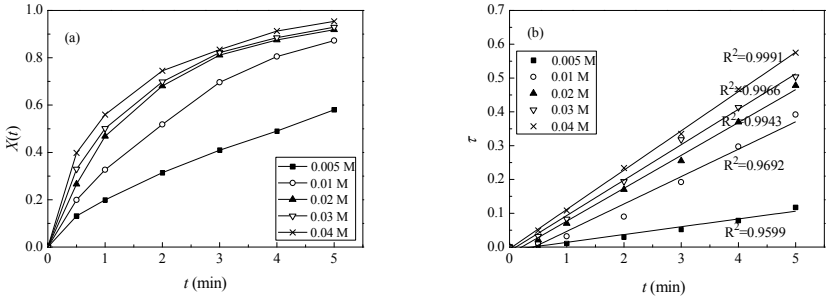

Fig. 3. Effect of initial Mg(II) concentration on ion exchange of Mg(II) with 732-CR (a) *X*(*t*) *versus t* and (b) *τ versus t* (temperature: 308 K)

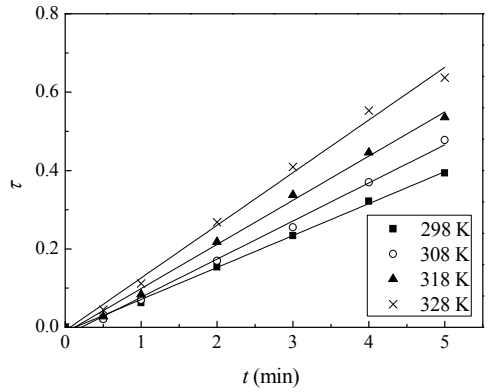

Fig. 4. Plots of *τ* versus *t* for ion exchange of Mg(II) with 732-CR at different temperatures

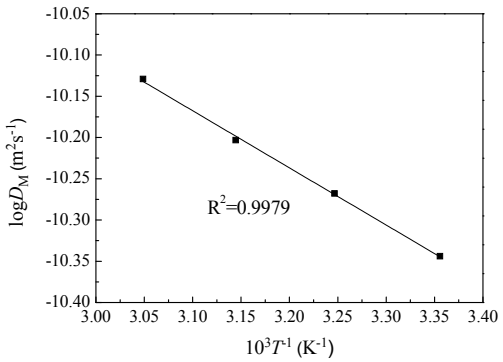

Fig. 5. Plot of log D_M versus 10^3T^{-1} for ion exchange of Mg(II) with 732-CR by Nernst-Planck equation

The entropy of activation (ΔS^*) is then calculated by substituting D_0 in following equation [29]:

$$D_0 = 2.72d^2\left(\frac{kT}{h}\right)\exp\left(\frac{\Delta S^*}{R}\right) \quad (11)$$

where *d* is the ionic jump distance taken as 5×10^{-10} m, *k* is the Boltzmann constant, *h* is Plank's constant and *T* is taken as 273 K. The ΔS^* values are summarized in Table 4.

Table 2. Slopes of various *τ* versus *t* plots (S_1) and $F_2(t)$ versus *t* plots (S_2) for ion exchange of Mg(II) with 732-CR at different temperatures

T (K)	298K	308K	318K	328K
$S_1(s^{-1}) \times 10^3$	1.36	1.62	1.88	2.23
$S_2(s^{-1}) \times 10^3$	1.72	2.03	2.34	2.71

3.2.2 Shrinking-core model

The shrinking core model (SCM) was also applied in order to interpret the experimental kinetic results better. In this model, it was assumed that: The process is isothermal; intraparticle mass transfer takes place by diffusion inside pores; and the resin particles are spherical with uniform size and density[30]. The SCM considers the exchange reaction of metal ions with the resins carried out from the surface to the centre of resin particles as the time passed. During the ion exchange process, a moving boundary between the reacted outer shell and the shrinking unreacted inner core can be observed during the ion exchange process [31].

Ion exchange of Mg(II) with 732-CR, as in other heterogeneous reactions between solids and fluids, can be explained through three sequential processes: 1) diffusion of ions through a boundary film around the resin particle (film diffusion); 2) diffusion of ions within the resin particle (particle diffusion); 3) exchange reaction with the functional groups attached to the matrix. One of the steps can be considered as the rate controlling step if it offers much greater resistance than the others. Assuming a quasi-steady state, the following relationships can be obtained when film diffusion or particle diffusion or exchange reaction is the rate controlling step, respectively [32,33].

$$F_1(t) = X \quad (12)$$

$$F_2(t) = 1 - 3(1-X)^{2/3} + 2(1-X) \quad (13)$$

$$F_3(t) = 1 - (1-X)^{1/3} \quad (14)$$

where *X* is the fractional attainment of equilibrium.

The results of the liner regression of $F_i(t)$ *versus t* for the exchange of Mg(II) with 732-CR at 308K are shown in Table 3. A good linearity is obtained only for the plots of $F_2(t)$ against *t* (correlation coefficient R^2 > 0.99), confirming the ion exchange processes follows the particle diffusion controlling mechanism. As to particle diffusion controlling model, the resistance of film diffusion around the resin particles is negligible.

As the reaction progresses in the resin bead, the material balance of counter-ion M follows Fick's diffusion equation with spherical coordinates [34]. By the relationship between the concentration gradient of M at any shell radius *r* and r_c, the radius of the interface of unreacted core with the associated boundary and initial conditions, we can obtain:

$$V\frac{dC_M}{dt}=4\pi q_e r_c^2\frac{dr}{dt}=4\pi D_e\left[\frac{1}{(1/r_0)-(1/r_c)}\right]C_M \quad (15)$$

where r_0 is the initial radius of resin particle and r_c is the radius of the interface of unreacted core. D_e is the effective diffusion coefficient for binary ion exchange. q_e is the exchange capacity of the resin, which is calculated by the difference in initial and final metal content at equilibrium using the following relationship:

$$q_e=\frac{(C_{M,e}-C_{M,0})V}{W/\rho_s} \quad (16)$$

where V is the volume of the solution, W is the weight of dried 732-CR, and ρ_s is the density of dried resin.

When Eq. (15) is integrated and combined with Eq. (13), we can obtain,

$$F_2(t)=1-3(1-f)^{2/3}+2(1-f)=\frac{6D_eC_{M,0}}{q_er_0^2}\int_0^t\left(\frac{C_M}{C_{M,0}}\right)dt=\left(\frac{6D_eC_{M,0}}{q_er_0^2}\right)t \quad (17)$$

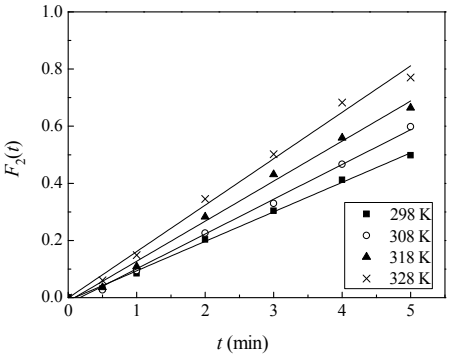

Fig. 6. Plot of $F_2(t)$ versus t for ion exchange of Mg(II) with 732-CR at different temperatures

While $F_2(t)$ is plotted against t, as shown in Fig. 6, we can calculate the effective diffusion coefficients D_e of Mg(II) according to the slopes of the lines, also listed in Table 2. The results of D_M and D_H (Nernst-Planck) and D_e (SCM) are listed in Tables 3.

On the basis of Eq. (10) and (11), self-diffusion coefficient of Mg(II) (D_0'), energy of activation (ΔE_a') and entropy of activation (ΔS^*') are obtained using the Arrhenius plot of log D_e *versus* $1/T$ (Fig. 7). The results are summarized in Table 3 along with the data obtained by Nernst-Planck method.

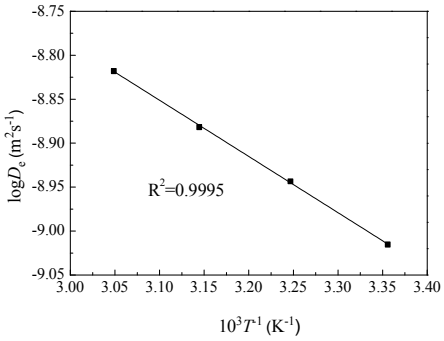

Fig. 7. Plot of logD_e versus 10^3T^{-1} for ion exchange of Mg(II) with 732-CR by shrinking-core model

3.2.3 Comparison between two kinetic models

As seen from Table 3, the values of D_e, D_M and D_H increase with the increase in temperature confirming that the mobility of the ions is bigger at a higher temperature in Fig. 2. The values of D_e are approximate that of D_H, but they are about 20 times as much as D_M. Considering the opposite direction of M^{2+} and H^+ diffusing in the resin phase, it is reasonable to think D_e is the characterization of the interaction of M^{2+} and H^+.

As is shown in Table 4, the positive values of ΔE_a and ΔE_a' indicate that a minimum energy is required to facilitate the ion exchange process. Negative values of ΔS^* and ΔS^*' suggest a greater degree of order is achieved during the exchange of Mg(II) with 732-CR, validating the feasibility of ion exchange processes on 732-CR.

Table 3. The correlation coefficient of $F_i(t)$ and values of D_M and D_H (Nernst-Planck) and D_e (SCM) for ion exchange of Mg(II) with 732-CR at different temperatures

Temperature	R^2			D_M	D_H	D_e
(K)	$F_1(t)$	$F_2(t)$	$F_3(t)$	(m^2/s)	(m^2/s)	(m^2/s)
298	0.8648	0.9979	0.9621	4.530×10^{-11}	6.342×10^{-10}	9.655×10^{-10}
308	0.8729	0.9968	0.9761	5.396×10^{-11}	7.554×10^{-10}	1.140×10^{-9}
318	0.8436	0.9941	0.9666	6.262×10^{-11}	8.766×10^{-10}	1.314×10^{-9}
328	0.8019	0.9927	0.9651	7.427×10^{-11}	1.040×10^{-9}	1.521×10^{-9}

Table 4. Values of D_0, ΔE_a and ΔS^* for ion exchange of Mg(II) with 732-CR by Nernst-Planck equation and D_0', ΔE_a' and ΔS^*' by shrinking-core model

Nernst-planck model			Shrinking-core model			D_0'/ D_0	α
D_0 (m^2/s)	Δ*E*a (kJ/mol)	Δ*S** (J/mol/K)	D_0' (m^2/s)	Δ*E*a' (kJ/mol)	Δ*S**' (J/mol/K)		
9.54×10^{-9}	5.76	-49.93	1.35×10^{-7}	5.32	-27.88	14.15	14

From Table 4, self- diffusion coefficients, D_0 and D_0', are approximately in the order of 10^{-8} m^2/s, which are essentially comparable to the literature results [35,36]. And the radios of D_0'/ D_0 for Mg(II) are in close proximity to α value, indicating that self-diffusion coefficient of H^+ (Nernst-Planck) equals to the effective self-diffusion coefficient (SCM). Hence, the application of both Nernst-Planck equation and shrinking-core model to solve the ion exchange kinetics of Mg(II) with 732-CR is ascertained.

4. CONCLUSIONS

The concentration effects on the rate of ion exchange of Mg(II) with 732-CR were studied and the results show that the ion exchange processes at various temperatures are favored under particle diffusion control mechanism when $C_{M,0}$ is larger than 20 mol·m^{-3}. The kinetics of Mg(II) on 732-CR were described by Nernst-Planck equation and shrinking-core model. Both kinetic models yielded a good fit for the kinetic data. Diffusion coefficients of counter ions (D_M and D_H) and effective diffusion coefficients of metal ions (D_e) within the resin were evaluated by above two kinetic models, respectively. The relationship between them reveals that D_e is the characterization of the interaction of M^{2+} and H^+. Positive values of energy of activation (ΔE_a) and negative values of entropy of activation (ΔS^*) were obtained, validating the feasibility of ion exchange processes.

COMPETING INTERESTS

Authors have declared that no competing interests exist.

REFERENCES

1. Zhi SL, Zhang ST. A novel combined electrochemical system for hardness removal. Desalination. 2014;349:68-72.
2. Pan YD, Si FQ, Xu ZG, Romero CE. An integrated theoretical fouling model for convective heating surfaces in coal-fired boilers. Powder Technol. 2011;210:150-156.
3. Indarawis KA, Boyer TH. Superposition of anion and cation exchange for removal of natural water ions. Sep. Purif. Technol. 2013;118:112-119.
4. Arias-Paic M, Cawley KM, Byg S, Rosario-Ortiz FL. Enhanced DOC removal using anion and cation ion exchange resins. Water Res. 2016;88:981-989.
5. Zarga Y, Boubaker HB, Ghaffour N, Elfil H. Study of calcium carbonate and sulfate co-precipitation. Chem. Eng. Sci. 2013;96:33-41.
6. Lin NH, Shih WY, Lyster E, Cohen Y. Crystallization of calcium sulfate on polymeric surfaces. J. Colloid Interf. Sci. 2011;356:790-797.
7. Brastad KS, He Z. Water softening using microbial desalination cell technology. Desalination. 2013;309:32-37.
8. Osorio KLV, Oliveira W, El Seoud AO. Hard water and soft soap: Dependence of soap performance on water hardness. A classroom demonstration. J. Chem. Educ. 2005;82:257-259.
9. Yu ZH, Qi T, Qu JK, Wang LN, Chu JL. Removal of Ca(II) and Mg(II) from potassium chromate solution on amberlite IRC 748 synthetic resin by ion exchange. J. Hazard. Mater. 2009;167:406-412.
10. Pakdehi SG, Alipour M. Adsorption of Cr(III) and Mg(II) from hydrogen peroxide aqueous solution by amberlite IR-120 synthetic resin. Iran. J. Chem. Chem. Eng. 2013;32:49-55.
11. Arugula MA, Brastad KS, Minteer SD, He Z. Enzyme catalyzed electricity-driven water softening system. Enzyme Microb. Technol. 2012;51:396–401.
12. Setiawan L, Shi L, Wang R. Dual layer composite nanofiltration hollow fiber membranes for low-pressure water softening. Polymer. 2014;55:1367-1374.
13. Liao Z, Gu Z, Schulz MC, Davis JR, Baygents JC, Farrell J. Treatment of

cooling tower blowdown water containing silica, calcium and magnesium by electrocoagulation. Water Sci. Technol. 2009;60:2345-2352.

14. Pramanik BK, Thangavadivel K, Shu L, Jegatheesan V. A critical review of membrane crystallization for the purification of water and recovery of minerals. Rev. Environ. Sci. Biotechnol. 2016;15:411–439.
15. Hakizimana JN, Gourich B, Vial Ch, Drogui P, Oumani A, Naja J, Hilali L. Assessment of hardness, microorganism and organic matter removal from seawater by electrocoagulation as a pretreatment of desalination by reverse osmosis. Desalination. 2016;393:90–101.
16. Xue ZT, Li ZL, Ma JH, Bai X, Kang YH, Hao WM, Li RF. Effective removal of Mg^{2+} and Ca^{2+} ions by mesoporous LTA zeolite. Desalination. 2014;341:10-18.
17. Bergman RA. Membrane softening versus lime softening in Florida: A cost comparison update. Desalination. 1995; 102:11–24.
18. Lito PF, Aniceto JPS, Silva CM. Removal of anionic pollutants from water and wastewaters and materials perspective for their selective sorption. Water Air Soil Pollut. 2012;223:6133–6155.
19. Picart S, Ramiere I, Mokhtari H, Jobelin I. Experimental characterization and modelization of ion exchange kinetics for a carboxylic resin in infinite solution volume conditions. Application to monovalent-trivalent cations exchange. J. Phys. Chem. B. 2010;114:11027-11038.
20. Perez-Gonzalez A, Ibanez R, Gomez P, Urtiaga AM, Ortiz I, Irabien JA. Recovery of desalination brines: Separation of calcium, magnesium and sulfate as a pre-treatment step. Desalin. Water Treat. 2015;56:3617-3625.
21. Guo H, Ren YZ, Sun XL, Xu YD, Li XM, Zhang TC, Kang JX, Liu DQ. Removal of Pb^{2+} from aqueous solutions by a high-efficiency resin. Appl. Surf. Sci. 2013;283: 660-667.
22. AlOthman ZA, Alam MM, Naushad M. Heavy toxic metal ion exchange kinetics: Validation of ion exchange process on composite cation exchanger nylon 6,6 Zr(IV) phosphate. J. Ind. Eng. Chem. 2013; 19:956-960.
23. Khan AA, Habiba U, Shaheen S, Khalid M. Ion-exchange and humidity sensing properties of poly-o-anisidine Sn(IV) arsenophosphate nano-composite cation-exchanger. J. Environ. Chem. Eng. 2013;1: 310-319.
24. Varshney KG, Gupta P, Tayal N. Kinetics of ion exchange of alkaline earth metal ions on acrylamide cerium(IV) phosphate: A fibrous ion exchanger. Colloid Surface B. 2003;28:11-16.
25. AL-Othman ZA, Inamuddin, Naushad M. Forward (M^{2+}−H^{+}) and reverse (H^{+}−M^{2+}) ion exchange kinetics of the heavy metals on polyaniline Ce(IV) molybdate: A simple practical approach for the determination of regeneration and separation capability of ion exchanger. Chem. Eng. J. 2011;171: 456-463.
26. Talha M, Naushad M. Ion exchange kinetics of heavy metal ions on organic–inorganic composite cation exchanger poly-o-toluidine Zr(IV) tungstate. J. Inorg. Organomet. Polym. 2012;22:822-829.
27. Helfferich F, Plesset MS. Ion exchange kinetics: A nonlinear diffusion problem. J. Chem. Phys. 1958;28:418-424.
28. Plesset MS, Helfferich F, Franklin JN. Ion exchange kinetics: A nonlinear diffusion problem. II. Particle diffusion controlled exchange of univalent and bivalent ions. J. Chem. Phys. 1958;29:1064-1069.
29. Bansal OP. Kinetics of ion-exchange on sodium-, calcium-, and magnesium saturated kaolinites. Bull. Chem. Soc. Jpn. 1983;56:1532-1535.
30. Fernandes S, Gando-Ferreira LM. Kinetic modeling analysis for the removal of Cr(III) by Diphonix resin. Chem. Eng. J. 2011;172: 623-633.
31. Dicinoski GW, Gahan LR, Lawson PJ, Rideout JA. Application of the shrinking core model to the kinetics of extraction of gold(I), silver(I) and nickel(II) cyanide complexes by novel anion exchange resins. Hydrometallurgy. 2000;56:323-336.
32. Fermindez A, Diaz M, Rodrigues A. Kinetic mechanisms in ion exchange processes. Chem. Eng. J. 1995;57:17-25.
33. Lin LC, Juang RS. Ion-exchange kinetics of Cu(II) and Zn(II) from aqueous solutions with two chelating resins. Chem. Eng. J. 2007;132:205-213.
34. Cortina JL, Warshawsky A, Kahana N, Kampel V, Sampaio CH, Kautzmann RM. Kinetics of goldcyanide extraction using

ion-exchange resins containing piperazine functionality. React. Funct. Polym. 2003;54: 25–35.

35. Agrawal A, Sahu KK, Rawat JP. Kinetic studies on the exchange of bivalent metal ions on amberlite IRC-718 - an iminodiacetate resin. Solvent. Extr. Ion. Exc. 2003;21:763-782.

36. Monazam ER, Shadle LJ, Siriwardane R. Equilibrium and absorption kinetics of carbon dioxide by solid supported amine sorbent. AIChE J. 2011;57:3153-3159.

Peer-review history:
The peer review history for this paper can be accessed here:
http://sciencedomain.org/review-history/16703